versity of Texas. Thanks are due to the staff of that institution, as well as to Drs. H. E. Morris and W. H. Lane of Monsanto's Texas Division, for their help and comments.

NOTATION

D = column diameter, in. or ft.
E_{OG} = absorption efficiency = $(y_1 - y_2)/y_1$
G_o = superficial gas mass velocity, lb./hr.-sq.ft.
G_M = superficial gas molar velocity, lb.-moles/hr.-sq.ft.
H = Henry's law constant, atm./mole fraction
k_La = volumetric liquid phase mass transfer coefficient, lb.-moles/hr.-cu.ft.-mole fraction
K_Ga = volumetric overall mass transfer coefficient based on gas phase, lb.-moles/hr.-cu.ft.-atm.
L = nongas flow submergence, in. or ft. of liquid
L/D = submergence/diameter ratio
N_{OG} = number of overall transfer units based on gas phase, dimensionless
y = mole fraction of oxygen in air
Z_f = observed height of aerated mass, in. or ft.
Z_L = equivalent height of clear liquid (also L), in. or ft.
π = total pressure, atm.

LITERATURE CITED

1. American Institute of Chemical Engineers, "Tray Efficiencies in Distillation Columns," Fourth Annual Progress Report, pp. 9 and 45, New York (June 30, 1956).
2. Cooper, C. M., G. A. Fernstrom, and S. A. Miller, *Ind. Eng. Chem.*, **36**, 504 (1944).
3. Davidson, L., and E. H. Amick, *A.I.Ch.E. Journal*, **2**, 337 (1956).
4. Elsworth, R., V. Williams, and R. Harris-Smith, *J. Appl. Chem.*, **7**, 269 (1957).
5. Foust, H. C., D. E. Mack, and J. H. Rushton, *Ind. Eng. Chem.*, **36**, 517 (1944).
6. Ragatz, E. G., and H. A. Baxter, *Oil and Gas J.*, **54**, No. 50, p. 158 (April 16, 1956).
7. Shulman, H. L., and M. C. Molstad, *Ind. Eng. Chem.*, **42**, 1048 (1950).
8. Siemes, W., and W. Weiss, *Chem.-Ing.-Tech.*, **29**, 727 (1957).
9. Willard, H. H., and N. H. Furman, "Elementary Quantitative Analysis," Van Nostrand, New York (1948).
10. Yoshida, F., A. Ikeda, S. Imakawa, and Y. Miura, *Ind. Eng. Chem.*, **52**, 435 (1960).

Manuscript received May 22, 1963; revision received August 17, 1964; paper accepted August 19, 1964. Paper presented at A.I.Ch.E. Buffalo meeting.

Kinetics of the Heterogeneous Decomposition of Iron Pentacarbonyl

HERBERT E. CARLTON and JOSEPH H. OXLEY

Battelle Memorial Institute, Columbus, Ohio

The decomposition of iron pentacarbonyl at pressures between one and 400 Torr was studied from 120° to 300°C. Up to about 200°C. the rate was primarily limited by surface kinetics of adsorbed carbonyl. Gas phase diffusional resistances were controlling at higher temperatures. In the kinetically controlled region the deposition rate was correlated by a Langmuir type of equation. Corrections for diffusion resistances in the kinetic region and kinetic resistances in the diffusion region were found to be appreciable.

A study of the thermal decomposition of iron pentacarbonyl was undertaken as part of a broad investigation of the basic mechanisms during the vapor deposition of solid materials. Iron pentacarbonyl was one reactant chosen for studying mass transfer characteristics. It decomposes in accordance with the overall equation:

$$Fe(CO)_5 \rightarrow Fe + 5CO \qquad (1)$$

The decomposition results in an unusually high molar ratio of products to reactants which should severely test the Stefan-Maxwell diffusion equations and mass transfer analogies, and the carbonyl decomposes at a low temperature which simplifies experimental techniques. Iron carbonyl is also especially suited for a study of combined kinetics and diffusion, since the decomposition is highly

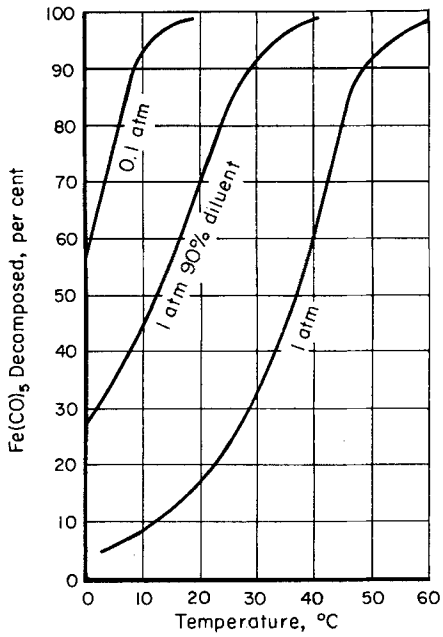

Fig. 1. Equilibrium decomposition of iron pentacarbonyl.

favorable thermodynamically in a region where the reaction proceeds at easily controlled rates (*1*). In order to investigate the diffusion rates, the chemical rate constants must be known to correct for residual kinetic effects. It is the purpose of this paper to summarize the results of the kinetic studies.

The previous work on the decomposition of iron carbonyl has largely been reported in the patent literature (*2* to *5*), and most of that work has been aimed toward the production of fine powders under conditions where the rate of chemical reaction was limited by nucleation and diffusion rather than by chemical kinetics. Schölzel (*5*) reports that the reaction proceeds step-by-step through iron nonacarbonyl and iron tetracarbonyl but presents no data that indicate the actual presence of these intermediates.

Several reviews of the physical, chemical ,and thermodynamic properties of iron carbonyl are available (*6*, *7*, *8*). Recently, Cotton, Fischer, and Wilkinson (*9*) reported on the heats of combustion and formation; Leadbetter and Spice (*10*) presented values for heat capacities and vapor pressures, and King and Lippencott (*11*) calculated the entropy, enthalpy, free energy, and heat capacity of the vapor from their Raman spectrum measurements. The authors have found no kinetic data for comparison with those presented in this paper.

THERMODYNAMIC ANALYSIS

The equilibrium data shown in Figure 1 were calculated from the best available information on the enthalpies and entropies of the system components (*9* to *12*). It can be seen that at temperatures above 50°C. the iron carbonyl is essentially completely converted under equilibrium conditions. It is believed that the temperature scale is reliable within at least 20°C. of the estimated values. Thus, since deposition usually does not occur at temperatures below about 120°C. (*1*), it should be safe to assume that there are no thermodynamic limitations on the deposition process at the temperature levels of interest, and the reverse of the deposition process, that is the reaction of carbon monoxide with iron, is negligible.

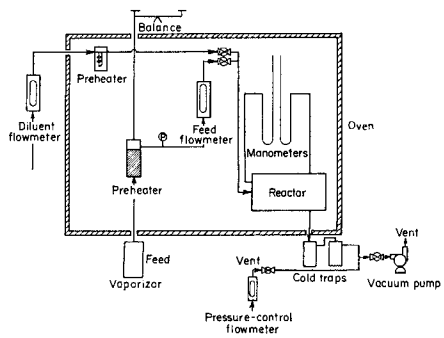

Fig. 2. Schematic diagram of equipment.

EXPERIMENTAL TECHNIQUES

Description of Equipment

A schematic diagram of the equipment is shown in Figure 2. The majority of the apparatus was located within an insulated box, which served as both a constant temperature oven to prevent condensation of the carbonyls and as a safety barrier to avoid possible health hazards should leaks occur during operation of the equipment. The oven was constructed of plywood, and insulating wallboard was mounted on the inside. The front of the box consisted of a double thickness of safety glass so that the experiment and instruments could be observed during a run. The oven was heated electrically with a forced circulation blower.

The reactor itself consisted of a 1½-ft. length of 5-in. diameter pipe flanged on both ends. A 5-in. diameter glass window was mounted on the downstream end to provide visual observation of the deposition process. A filament and a gas-directing orifice were mounted inside the reactor. Details of their construction are shown in Figure 3. The filaments were hollow steel tubes approximately 5½ in. long and had an outside diameter of ⅛ in. Deposition temperatures were measured with a 36-gauge chromel-alumel thermocouple inserted in the center of the hollow filaments. The filaments were resistively heated with 60-cycle electric power supplied through a variac and a 40:1 step-down transformer. The gas stream was directed over the filaments by a rectangular orifice, 3½ in. high and ½ in. wide.

The manufacturer of the iron pentacarbonyl claims better than 99.5% purity, with the major impurities being iron nonacarbonyl and iron oxides. Since neither of these impurities is volatile, the carbonyl vapor used should be purer than the supplied liquid. A spectroscopic analysis indicated only minor traces of metallic impurities.

The hydrogen used for these experiments was diffused through palladium before use. The other gases were of a com-

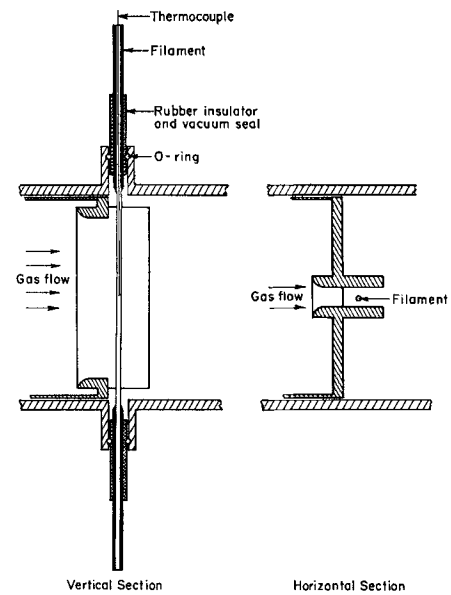

Fig. 3. Filament and orifice detail.

TABLE 1. DEPOSITION-RATE DATA

Experiment number	Deposition rate, g./sq. cm. hr.	Total pressure, Torr	Reynolds number	Deposition temperature, °C.	Diluent gas Volume, %	Species
72	0.12	1	21	150	0	
88	0.034	20	64	130	0	
95	0.016	20	20	150	55	CO
102	0.69	20	9	200	0	
81	0.90	208	200	200	0	
108	2.66	32	166	250	0	

mercially available high-purity grade sold in compressed gas cylinders and were used without further purification. The deposition element was a commercial grade of mild steel seamless tubing. Copper electrodes were silver soldered on the ends. The filaments were cleaned with steel wool and abrasive paper and polished with crocus cloth before use.

Explanation of Procedure

In preparation for an experiment, the filament was weighed and installed. All of the apparatus except the filament was brought up to operating temperature. The gases in the system were removed by a vacuum pump. Hydrogen was passed over the filament at a pressure of about 80 Torr, while the filament was rapidly heated to 530°C. and immediately cooled. The hydrogen flow was terminated, the system evacuated, and finally the carbonyl flow and diluent flow, if any, were started. The system pressure was increased to the desired value. The filament was then heated rapidly to the desired temperature by activating the electrical heating circuit. During the experiment, the various system parameters were monitored and recorded, and minor adjustments were made to maintain constant conditions. After the filament had cooled, the vacuum was broken with nitrogen or other inert gases, and the filament was replaced with another in preparation for the next experiment. The deposition rate was determined from the weight gain of the filament, the initial surface area of the filament, and the length of the run. The iron deposited on the filament outside of the 3½ in. length in the orifice was mechanically removed before weighing. A minor correction to the measured weight was made by estimating the weight deposited during cool down following a run. No correction was made for increase in filament diameter because of deposition, but the lengths of the runs were chosen so that the change in diameter was only about 2%.

Steel filaments were used to avoid possible complications of foreign substrates. However, in the early experiments, the deposits were discontinuous, consisting of islands of deposits widely separated from each other, and the data were not reproducible because of the variable surface area. The hydrogen pretreatment described was found to give much more uniform surface nucleation, and the data were reproducible to within a few per cent.

In no run was more than 15% of the iron carbonyl decomposed. The rate data were therefore analyzed on the basis of a differential reactor system, and the composition of the bulk gas stream flowing past the filament was assumed to the arithmetic average of the inlet and outlet compositions.

EXPERIMENTAL RESULTS

Samples of the deposition-rate data are presented in Table 1. The first three experiments illustrate conditions where chemical kinetics primarily control deposition rate, the next two experiments illustrate conditions where both kinetics and diffusion play important parts in controlling deposition rate, and the last experiment illustrates conditions where diffusion was the primary rate-controlling mechanism. Additional data are presented in the figures showing the effects of the individual variables.

By analogy, the mass transfer characteristics of the system should be similar to the heat transfer characteristics. A heat transfer study was therefore carried out to check the transfer characteristics of the orifice and filament geometry. The experimentally determined convective heat transfer coefficients were compared with the heat transfer correlation recommended by McAdams (*13*), and the results are shown in Figure 4. The experimental rates were corrected for radiation losses by assuming the emissivity of the filament to be 0.24, a value recommended by McAdams for iron freshly abraded with emery paper. Above a Reynolds number of about 20, the data agree very closely with the published correlation. However, at the low Reynolds numbers, the experimental heat transfer rates were high, possibly due to natural convection (*14*). The standard deviation of all the experimental Nusselt numbers from the values predicted by the McAdams correlation at a given Reynolds number was only 18%. Although the McAdams correlation was derived from data obtained with air, the difference in heat transfer characteristics on the basis of a Nusselt-Reynolds number correlation between air and hydrogen or argon should be small and less than the experimental error in these data or in the data used by McAdams.

In Figure 5, the deposition rate is plotted against the reciprocal temperature at three flow rates and at 20 Torr pressure. A similar plot could have been made at other pressures. At temperatures below about 200°C., the rate of deposition is very sensitive to temperature, while at higher temperatures the rate is relatively unaffected. This type of behavior is typical of a reaction which is controlled by chemical kinetics at low temperature and by gas-phase diffusion at high temperature.

The effect of pressure on deposition rate is shown in Figure 6. At 150°C., the reaction rate is decreased as the pressure of the iron pentacarbonyl is increased, suggesting strong adsorption of reactants and products by a multisite reaction mechanism. At higher temperatures, the rate becomes independent of pressure, which is characteristic of a diffusional-controlled process at constant Reynolds number.

The effect of flow rate is shown in Figure 7. Empirically the rate increases about as the 0.3 power of flow rate at 150° and 200°C. and as the 0.4 power of flow rate at 225° and 250°C. This increase in exponent would be expected as diffusional control became more important at the higher temperatures, but from the data it is difficult to determine if this increase is true or caused by data scatter. The analogy with heat transfer predicts an exponent of about 0.45 in this flow range, in good agreement with the data.

Figure 8 illustrates the effect of dilution of the iron carbonyl with helium, argon, and carbon monoxide. At 150°C., when inert diluents such as argon or helium were used, it was found that the addition of diluents to a constant-mass flow of iron carbonyl slightly increased the deposition rate. This resulted from a reduction of the partial pressure of the products and reactants and affected the deposition rate in the same way as a reduction of total pressure. This was not a Reynolds number effect, since Reynolds number was slightly reduced or remained con-

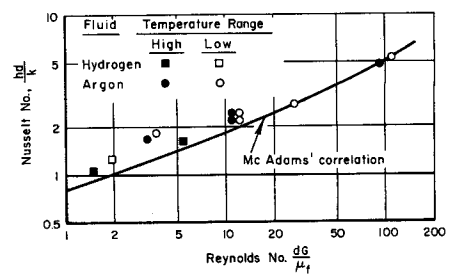

Fig. 4. Heat-transfer data.

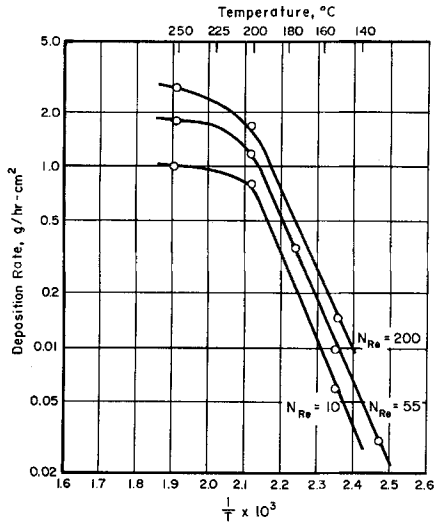

Fig. 5. Effect of temperature and Reynolds number on deposition rate at a pressure of 20 Torr.

stant when diluent was added as the higher viscosity of the diluent cancelled out the effect of increased mass flow. Carbon monoxide diluent markedly decreased the deposition rate. With 50 vol. % carbon monoxide in the deposition gas at 150°C., the rate was less than one-third the rate with undiluted iron carbonyl feed, despite the fact that equilibrium was not a limiting factor.

In the 200° to 250°C. temperature region, dilution of a constant stream of iron carbonyl with argon and helium slightly reduced the deposition rate. This reduction in rate was probably caused by a change in the diffusional characteristics of the system. Since diffusion through helium is faster than diffusion through argon, the reduction of the rate was less with helium additions. Only two points are available with carbon monoxide dilution. The point at 250°C. is on the argon line, as would be expected from the diffusional properties of carbon monoxide. This indicates that kinetics has a negligible effect at 250°C. At 200°C. the deposition rate with the carbon monoxide diluent is only about one-half of that when a corresponding amount of argon was used. This further confirms that kinetics affects deposition rate at 200°C.

The gross effects of the variables just described indicate that the chemical kinetics of the reaction primarily control the deposition rate at temperatures below about 200°C. The temperature sensitivity of the reaction and the variation in reaction rate with pressure are both characteristic of kinetic control. The sharp decrease in rate when carbon monoxide is added to the reaction gases is further confirmation of this assumption. However, the fact

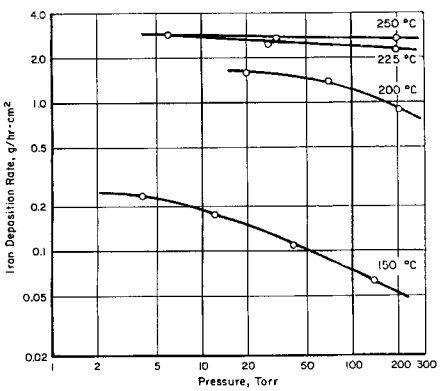

Fig. 6. Effect of pressure on deposition rate at constant flow rate ($N_{Re} \simeq 200$).

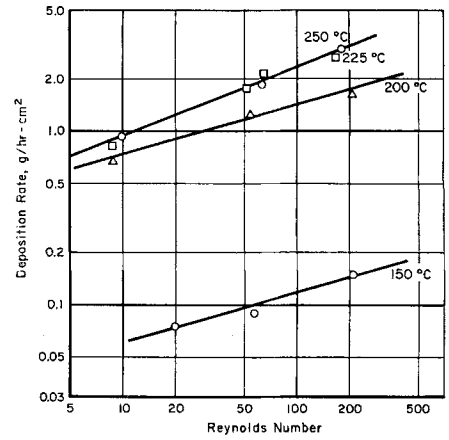

Fig. 7. Effect of flow rate on deposition rate at 20-Torr pressure.

that the deposition rate increases with increasing flow rate, even at very low conversions, and hence for essentially undiluted reactants in the bulk stream, indicates that there is a residual mass transfer effect even at this low temperature. The data for temperatures above 200°C. indicate that diffusion largely controls the deposition rate at these temperatures. There is little change in deposition rate with temperature above about 200°C., and the effect of pressure is negligible. These effects are characteristic of the diffusion-limited process. However, carbon monoxide dilution of the reactant at 200°C. reduces the deposition rate more than an equal amount of argon, indicating that there is a residual kinetic control of the deposition rate.

The upper temperature limit of applicability of these data was limited by gas-phase nucleation. Gas-phase nucleation occurs when iron carbonyl decomposes in the vapor phase rather than on the heated surface. At the temperature when gas-phase nucleation occurs, the appearance of the deposit changed from bright to black, and at a slightly higher temperature threads of fine precipitated iron were observed streaming back from the filament. Also, the deposition rate decreased erratically. The highest deposition temperature observed without gas-phase decomposition was slightly above 300°C. High temperatures for nucleation were observed at high pressures, high flow rates, and also at high carbon monoxide dilution. The addition of argon always decreased the nucleation temperature. The lowest observed gas-phase nucleation temperature, 225°C., was obtained with 87% argon dilution.

CORRELATION OF RESULTS

The deposition reaction was visualized as occurring in

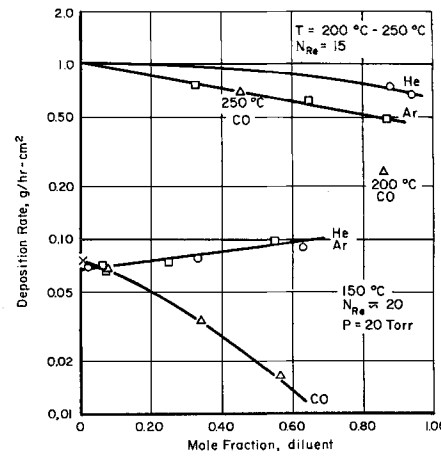

Fig. 8. Effect of diluent on deposition rate

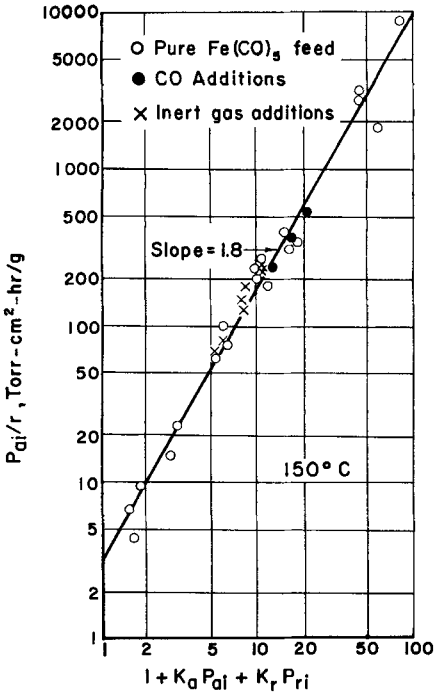

Fig. 9. Correlation for surface kinetics controlling.

a series of consecutive mass transfer and kinetic steps. The slowest step in the process then will control deposition rate.

In order to separate the kinetic steps from the mass transfer steps, the drop in partial pressure of reactants due to mass transfer effects was estimated. This estimate was made from the heat transfer correlation of McAdams (*13*) for gases passing over a cylinder in cross flow. The heat transfer correlation was converted for mass transfer by use of the Chilton-Colburn (*15*) analogy between heat transfer and mass transfer. The generalized equation for vapor-deposition rate under conditions of diffusion control on the basis of film theory is of the form

$$r = M_w k_y \Delta y \tag{2}$$

where (*16*)

$$\Delta y = \frac{1}{4} \ln \frac{P + 4P_a}{P + 4P_{ai}} \tag{3}$$

With experimentally determined deposition rates used, these equations were solved for the interfacial partial pressure P_{ai}.

In mathematically representing the three interfacial steps, it is generally necessary to assume that the other nonlimiting processes are at equilibrium. This is a rather severe assumption and possibly is not valid. However, the mathematics which include the simultaneous partial limitations of all three steps becomes rather unwieldly and impractical. The generalized correlating equations for each of these limiting processes are shown below, and it should be obvious that they are rather minor extensions of the Hougen and Watson (*17*) method for applying the Langmuir-Hinshelwood adsorption-surface reaction mechanism.

Adsorption limiting:

$$r = \frac{K_o (P_{ai} - P_{ri}^5/K_{eq})}{1 + (K_a/K_{eq}) P_{ri}^5 + K_r P_{ri} + K_i P_{ii}} \tag{4}$$

Surface reaction limiting:

$$r = \frac{K_o K_a (P_{ai} - P_{ri}^5/K_{eq})}{[1 + K_a P_{ai} + K_r P_{ri} + K_i P_{ii}]^n} \tag{5}$$

Desorption limiting:

$$r = \frac{K_o [(K_{eq} P_{ai})^{0.2} - P_{ri}]}{1 + K_a P_{ai} + K_a (K_{eq} P_{ai})^{0.2} + K_i P_{ii}} \tag{6}$$

Correlating coefficients were then found for each equation by a regression analysis of the 150°C. data. These analyses indicated that the reverse reaction was negligible in all cases as were the adsorption coefficients of argon and helium. Using the percentage standard deviation, that is one hundred times the square root of the sum of squares of the differences between the actual rates and calculated rates divided by the actual rates, as a figure of merit, one can judge the validity of the models on the basis of the degree of correlation of the appropriate equations. On this basis, the adsorption and desorption models were eliminated because the standard deviation of the data was greater than 100%. The surface reaction equation correlated the data reasonably well if the exponent was between 1.6 and 2.0, with a standard deviation of 28% for the best correlation at $n = 1.8$ as shown in Figure 9. However, at $n = 2.0$, the standard deviation was 29%, a statistically insignificant change.

The data from the experiments at 200° and 225°C. were then analyzed in the same manner for the surface-reaction equation with several values of n. The best results were obtained at n equal to 1.8, where the standard deviation was 46% in each case. Since the diffusion limitation accounts for much of the rate limitation in most experiments at 200° and at 225°C., a large standard deviation was expected and will not make the overall rate equation unduly inaccurate.

Table 2 presents the adsorption constants obtained from these analyses. Since on theoretical ground K_o, K_a, and K_r should be exponential functions of reciprocal temperature, the rate equation becomes

$$r = \frac{k_o k_a \exp^{-E_o/RT} \exp^{E_a/RT} (P_{ai} - P_{ri}^5/K_{eq})}{(1 + k_a \exp^{E_a/RT} P_{ai} + k_r \exp^{E_r/RT} P_{ri})^{1.8}} \tag{7}$$

and the recommended correlating constants determined from the values shown in Table 2 are

$k_o = 2.7 \times 10^{10}$ g./(hr.) (sq.cm.)
$k_a = 1.2 \times 10^{-3}$ Torr^{-1}
$k_r = 1.0 \times 10^{-11}$ Torr^{-1}
$E_o = 20{,}200$ cal./g.-mole
$E_a = 4{,}800$ cal./g.-mole
$E_r = 21{,}500$ cal./g.-mole

The constant in the exponential term for the adsorption constant of iron carbonyl E_a can be interpreted as the heat of adsorption of iron carbonyl on iron. The value of 4,800 cal./g.-mole indicates that the adsorption is physical on Van der Waals. However, the value of 21,500 cal./g.-mole for carbon monoxide indicates chemisorption. This value is in relatively good agreement with a direct measurement of 17,000 to 23,000 cal./g.-mole made by Beebe and

Table 2. Coefficients of Rate Equations at Various Temperatures

$$r = \frac{K_o K_a P_{ai}}{(1 + K_a P_{ai} + K_r P_{ri})^{1.8}}$$

Reactor temp., °C.	$K_o K_a$	K_a	K_r	Std. Dev., %
150	0.29	0.25	1.28	28
200	9.3	0.16	0.27	46
225	7.8	0.18	0.04	46

Stevens (*18*) at 0°C. The adsorption constants for argon and helium were found to be essentially zero over the range of temperature of interest.

The exponent n can have several theoretical explanations. Hougen and Watson (*17*) indicate that it should be an integer, and if the value is 2, they indicate that two sites are involved in the surface reaction. An exponent of 2 will fit the data almost as well as the exponent 1.8. Another interpretation is that n indicates the number of adsorbed carbon monoxide molecules per molecule of carbonyl after the surface reaction is completed. This mechanism can be supported by a heat balance, since the heat of reaction of the adsorbed species is about the amount required to desorb three molecules of carbon monoxide. A third explanation is that the adsorbed carbon monoxide requires about twice the surface area of adsorbed carbonyl. This agreement can be supported by simple geometric considerations.

By examination of the correlating equation, it becomes apparent why there is a negative effect of carbonyl pressure, and also why there is considerable effect of mass transfer in the kinetically controlled region. The negative effect of carbonyl pressure is caused by the pressure terms to approximately the second power in the denominator, while the pressure term in the numerator is only to the first power. Therefore, when pressure is increased, the rate is decreased. The effect of mass transfer is greatly accentuated owing to the sensitivity of the deposition rate to adsorbed carbon monoxide. A mass transfer resistance, which has only a minor effect on the partial pressure of carbon monoxide at the interface, can have a large effect on deposition rate. In addition, the flow rate also establishes the level of carbon monoxide in the bulk stream, which is likewise reflected at the interface.

CONCLUSIONS

1. The deposition rate of iron from its carbonyl is affected by both diffusion and chemical kinetics. At temperatures below about 200°C., chemical kinetics is usually the major factor in limiting the deposition rate, while at higher temperatures gaseous diffusion is usually the major factor in limiting the deposition rate.

2. The rate-limiting step in the chemical reaction is the decomposition of adsorbed iron carbonyl on the deposition surface, and the activation energy of the decomposition reaction of carbonyl is about 20,000 cal./g.-mole.

3. The carbonyl is apparently only weakly adsorbed, with a heat of adsorption of about 5,000 cal./g.-mole, and owing to the stoichiometry of the adsorption reaction, it has a negative effect on the reaction rate in the range of practical interest.

4. Carbon monoxide is quite strongly bonded to the iron surface, with a heat of adsorption of about 22,000 cal./g.-mole, and therefore strongly suppresses the deposition rate despite the favorable thermodynamics in the range of practical interest.

5. Argon and helium are adsorbed on iron much less strongly than iron carbonyl or carbon monoxide, and their presence does not affect the chemical kinetics except as they change the partial pressure of the reactants.

ACKNOWLEDGMENT

The authors wish to express their appreciation to the many companies cooperatively sponsoring the fundamental program on Chemical Vapor Deposition at Battelle for their financial support. We wish to thank Dr. J. M. Blocher, Jr., and Mr. A. C. Loonam who encouraged and contributed to this work, Mr. A. E. Cover who assisted in the experimental phase of the program, and Mr. F. G. Wise and Mrs. J. V. Bossenbroek who assisted in computer programing.

NOTATION

d = filament diameter, cm.
E_a = carbonyl adsorption energy, cal./g.-mole
E_o = activation energy, cal./g.-mole
E_r = carbon monoxide adsorption energy, cal./g.-mole
G = mass flow rate, g./hr.-sq.cm.
h = heat transfer coefficient, cal./hr.-sq.cm. °K.
K_a = adsorption constant for iron carbonyl, $Torr^{-1}$
K_{eq} = equilibrium constant of iron carbonyl decomposition, $3.34 \times 10^{11} \exp(24{,}850/T + 16.06 \log_{10} T - 1.76 \times 10^{-3} T - 3.032 \times 10^{5}/T^2)$, $Torr^4$
K_i = adsorption constant for inert, $Torr^{-1}$
K_o = rate constant, g./hr.-sq.cm.
K_r = adsorption constant for carbon monoxide, $Torr^{-1}$
k = thermal conductivity, cal./cm.hr.°K.
k_a = iron carbonyl adsorption coefficient, $Torr^{-1}$
k_g = mass-transfer coefficient, g.moles/sq.cm.-hr.
k_o = rate coefficient, g./hr.sq.cm.
k_r = carbon monoxide adsorption coefficient, $Torr^{-1}$
M_w = atomic weight of iron, 55.85 g./g.-atom
N_{Re} = Reynolds number, dG/μ_f
n = exponent in kinetic equation
P = total pressure, Torr
P_a = partial pressure of iron carbonyl, Torr
P_{ai} = partial pressure of iron carbonyl at interface, Torr
P_{ii} = partial pressure of inert component at interface, Torr
P_{ri} = partial pressure of carbon monoxide at interface, Torr
R = gas constant, cal./g.-mole°K. or cc. Torr/g.-mole °K.
r = deposition rate, g./hr.sq.cm.
T = temperature, °K.
Δy = diffusion potential
μ_f = viscosity of gas film, g./cm.-hr.

LITERATURE CITED

1. Powell, C. F., I. E. Campbell, and B. W. Gonser, "Vapor Plating," Wiley, New York (1955).
2. Beller, Hans, *U.S. Pat. 2,597,701* (1952).
3. Altman, G. O., *U.S. Pat. 2,612,440* (1952).
4. Beller, Hans, *U.S. Pat. 2,674,528* (1954).
5. Scholzel, Karl, *U.S. Pat. 2,919,207* (1959).
6. Antara Chemicals, "Iron Pentacarbonyl," New York (1953).
7. Merkel, Karl, "Uber die reinen Eisencarbonyle," Office of the Publication Board, Department of Commerce BP256-33S5, Washington, D. C. (1941).
8. Belozerskiy, N. A., "Karbonily Matallov," Moscow, Russia (1958).
9. Cotton, F. A., A. K. Fischer, and G. Wilkinson, *J. Am. Chem. Soc.*, **81**, 800 (1959).
10. Leadbetter, A. J., and J. E. Spice, *Can. J. Chem.*, **36**, 1923 (1959).
11. King, F. T., and E. J. Lippencott, *J. Am. Chem. Soc.*, **78**, 4192 (1956).
12. Wicks, C. E., and F. E. Block, *Bureau of Mines Bulletin 605*, Washington, D. C. (1963).
13. McAdams, W. H., "Heat Transmission," 3 ed., McGraw-Hill, New York (1954).
14. White, R. R., and S. W. Churchill, *A.I.Ch.E. Journal*, **5**, 354 (1959).
15. Chilton, T. H., and A. P. Colburn, *Ind. Eng. Chem.*, **26**, 1183 (1934).
16. Sherwood, T. K., "Absorption and Extraction," 1 ed., McGraw-Hill, New York (1937).
17. Hougen, O. A., and K. M. Watson, "Chemical Process Principles," Part 3, Wiley, New York (1947).
18. Beebe, R. A., and N. P. Stevens, *J. Am. Chem. Soc.*, **62**, 2134 (1940).

Manuscript received April 13, 1964; revision received September 9, 1964; paper accepted September 11, 1964.